Finite Elements in Analysis and Design 47 (2011) 78–84

Contents lists available at ScienceDirect

Finite Elements in Analysis and Design

journal homepage: www.elsevier.com/locate/finel

Numerical modelling of the Young's modulus of syntactic foams

F.V. Antunes [a], J.A.M. Ferreira [a,*], C. Capela [b]

[a] University of Coimbra, Mechanical Engineering Department, CEMUC, Polo II da Universidade de Coimbra, Pinhal de Marrocos, 3030-788 Coimbra, Portugal
[b] Polytechnic Institute of Leiria, Mechanical Engineering Department, CDRsp, Morro do Lena, Alto Vieiro, 2400-901 Leiria, Portugal

ARTICLE INFO

Article history:
Received 9 February 2010
Received in revised form
7 September 2010
Accepted 11 September 2010
Available online 30 October 2010

Keywords:
Syntactic foam
Finite element method
Young's modulus
Sensitivity analysis
Epoxy

ABSTRACT

Syntactic foams are particulate composites obtained by filling a polymeric matrix with hollow solid inclusions. Numerical simulations are an important tool to predict material behaviour and optimize the mechanical properties. The aim of this work is to develop a multi-phase numerical model to predict stiffness of the syntactic foams. The numerical parameters were identified and optimized, and the numerical predictions were validated with experimental results from 3-point bending tests. Different physical parameters were then studied, namely the volume fraction and the size of the filler, the elastic properties of filler and matrix and the inclusion's thickness. A sensitivity analysis was developed to quantify the importance of these different parameters, and the rigidity of the matrix was found to be the most influent. The parametric space was scanned and a numerical interpolation procedure implemented based on shape functions of finite element method. The procedure is an interesting tool for design and was used to identify the particles having stiffness equal to the matrix.

1. Introduction

Composite materials of polymeric matrix reinforced with particles may present interesting properties and have been replacing conventional engineering materials in a wide range of applications. Particles are easily mixed with the liquid matrix resin, and the mixture can be injection or compression moulded to produce components with complicated shapes. Filling particles are usually stiffer and more resistant than the matrix. Syntactic foams are obtained by filling a polymeric matrix with hollow micro-spheres, most often approximately or exactly spherical shaped. Spherical shape allows for the best packing factor and hydrostatic compression strength [1]. Syntactic foams are preferred to standard low density foams when high specific mechanical properties are required, rather than just low density [2]. The hollow spheres used in the syntactic foams have a diameter in the range 1–500 μm with a wall thickness between 0.5 and 4 μm [1]. The spheres are typically glass micro bubbles, which have an excellent mechanical strength, a smooth regular surface and good wetting characteristics. All of these qualities combine to create a well-established low cost production process. Thermosetting polymers as opposed to thermoplastic polymers are normally the preferred binders, due to the easier manufacturing technologies. The properties of the resulting syntactic foam are more directly tied to filler type and filler/binder interaction [1]. Syntactic foams have many advantages over most other materials such as: demonstrated superior compressive properties, low density, low dielectric constant and magnetic permeability, low radar detectability, very machinability, high rigidity, low thermal expansion, good thermal and water insulation properties, low conductivity, no corrosion effects, resistance to crack propagation, excellent creep performance, fire resistance, low moisture absorption and adaptability to a wide range of environment and service conditions. Low-density sheet moulding compounds based on hollow glass micro-spheres are being increasingly used in automotive, aeronautical and marine applications, namely underwater buoyancy aids, structural components such as hulls and bulkheads of ships and submarines. Syntactic foams are also potentially good materials for applications where impact loads occur [3], which can be an important parameter in design or the selection of materials. Syntactic foams are frequently used as core materials in sandwich configurations in consequence of their superior properties and ability to keep the damage highly localized, becoming more damage tolerant structures than other conventional core materials.

The design and development of high-performance materials requires the understanding and careful control of microstructure and its effect on properties. Numerical simulations of rigidity, damage and fracture of composites are an important tool to predict material behaviour and optimize the mechanical properties. Syntactic foams are macroscopically isotropic materials due to the randomness microspheres distribution, composed by two or three phases depending on whether additional voids are dispersed between the matrix binder and the microspheres. Three-dimensional numerical simulations of statistically representative

* Corresponding author. Tel.: +351 239 790755; fax: +351 239 790701.
E-mail addresses: fernando.ventura@dem.uc.pt (F.V. Antunes), martins.ferreira@dem.uc.pt (J.A.M. Ferreira), ccapela@estg.ipleiria.pt (C. Capela).

0168-874X/$ - see front matter © 2010 Elsevier B.V. All rights reserved.
doi:10.1016/j.finel.2010.09.007

micro-heterogeneous material samples are required to obtain realistic predictions. The 3D models with different complexity levels can be found in the literature. The simplest and most widely used models consist of a unit cell with matrix and reinforcement, assuming regular packing of the particles. It is assumed that the composite is made of an array of basic units, each with identical composition, geometry and material properties. Different topologies have been assumed [4], namely simple cubic [5] or face centred [6]. The face centred cell array enables the maximum packing efficiency of 0.74 particle volumetric fraction (PVF) in comparison with the maximum PVF for simple cubic particle array (0.523), for spheres of equal radius. These models are adequate to study the influence of geometrical parameters (particle radius, particle size, particle shape, etc.) and material parameters on the properties of the composite. The incorporation of a soft interface around particles has also been modelled with simple cubic models [5]. However, the study of particle distribution and clustering requires models with several particles. Drugan and Willis [7], Drugan [8] and Kari et al. [9] demonstrated that the size of the representative volume element (RVE) was unexpectedly small in the statistical sense. This means that estimates obtained with a few dozen spheres in an RVE presented very little scatter and that the average values of the elastic moduli gathered from the simulation of different representative volumes were very close. Segurado et al. [10–12], considered 30 particles, with random distribution, while Mishnaevsky [13] considered up to 15 particles. They found that the inhomogeneities in the particle spatial distribution had a negligible influence on the effective composite properties in the elastic and plastic regimes, but may affect the strength of the composite. However, the models with several particles present relatively complex challenges and are computationally demanding. Others aspects have been studied with single-particle and multi-particle models, namely, decohesion of particles [14–16], non-spherical particles [17] and viscoplasticity [18]. Replication of real particle composites has also been developed from micrographs of different material layers [19,20]. The mechanical behaviour of syntactic foams have been studied using analytical [2,21] and numerical approaches. Bardella et al. [2] considered a 2D axisymmetric finite element model of one unit cell. Rizzi et al. [1] studied syntactic foam and developed a model considering a modified Drucker–Prager elastic–plastic behaviour for the matrix. A detailed analysis of the elastic behaviour of syntactic foams, including a sensitivity analysis, focused on geometrical and material parameters, using 3D numerical multi-phase models with one or several particles has not been reported.

The aim of the present work is to develop a multi-phase numerical model to predict the stiffness of syntactic foams. The model consisted of a simple cubic cell and was used to study the effect of volumetric fraction, filler's size, thickness of hollow spheres and elastic properties of filler and matrix. Experimental work was developed in order to validate this numerical model. An empirical model, based on shape functions of the finite element method, was defined to interpolate the numerical results. The effect of particle's relative position was studied with a two particle model.

2. Experimental work

Syntactic foams were manufactured using hollow micro-spheres Verre ScotchitTM-K20 produced by 3 M. According to the manufacturer, the average diameter of the particles is 60 μm, 10% of particles have diameters lower than 30 μm, 10% of particles have diameters higher than 90 μm and the maximum size is 105 μm. The average density of particles is 200 kg/m^3. The resins used for binding micro-spheres, consisted of an epoxy 520 with hardener 523 and polyester Hetron 92 FR supplied by Ashland Chemical Hispania. Resins and hardener were mixed in a pot and then a predetermined amount, dependent on an intended volume fraction, of micro-spheres was added while stirring. Composite sheets were manufactured using an aluminium mould with a rectangular parallelepiped cavity of $400 \times 200 \times 6$ mm^3. The mould was cleaned using acetone and treated with release agent fluid green, MCP. Rectangular parallelepiped specimens were cut from the moulded plates with dimensions of $65 \times 12 \times 6$ mm^3 for flexural tests. These tests were performed according to ASTM D790-98, at 1 mm/min load rate, by using a Shimadzu AG-10 10 kN universal testing machine, equipped with a 1 kN load cell and TRAPEZIUM X software. The load versus displacement curves were obtained directly and the stresses were calculated by using linear elastic bending beam relationships. The bending Young's modulus was obtained by the linear elastic bending beams theory relationship

$$E = \frac{\Delta P L^3}{48 \Delta u I} \quad (1)$$

where L is the beam span, I is the inertia moment of the transverse section, and ΔP and Δu are, respectively, the load range and flexural displacement range at mid-span in the linear region of load versus displacement plot. The stiffness value was calculated by linear regression on the stress versus strain record, ranged from zero to a defined strain value. The value obtained depends on the maximum strain used to define the segment size. The maximum segment giving a linear regression correlation factor of at least 99% was considered. For each test condition, at least five specimens were tested.

Fig. 1a shows typical stress–displacement curves obtained in flexural tests for different filler contents. A brittle behaviour characterized by a linear load versus displacement curve almost until the failure was observed in all filled materials, in spite of the plastic behaviour of the epoxy neat resin. Fig. 1b shows the average values and the standard deviation of Young's modulus, obtained from Eq. (1), against the filler content. A significant decrease of both failure stress and flexural stiffness with the glass microsphere content was observed. These two mechanical properties showed lower values for polyester than for epoxy resin composites. Despite the absolute values of the stiffness modulus show a significant decrease (nearly linear) with the microsphere volume fraction, the specific values increase with filler content. This could be an advantage for the use of these materials as they show a gain of stiffness for the same weight. Fig. 2a is a SEM image of the morphological features of mode I fracture surfaces for specimens manufactured with an epoxy resin and V_f=26%. The picture shows a low presence of micro-porosities and a brittle fracture with low matrix deformation. Apparently the particles are homogeneously distributed, with no indication of clustering, which has a detrimental effect on composite strength [11]. In agreement with failure mechanisms reported in literature, significant pull out of the microspheres was observed together with some fracture. Fig. 2b is a detail of a broken hollow particle. The thickness of the hollow sphere is about 0.37 μm, which is slightly below the lowest values reported in the literature.

3. Numerical model

Fig. 3a illustrates the mid-section of the 3D physical model considered in the numerical analysis of the cubic simple cell. This is a simple multi-scale model that uses a simplified approach to the material's complexity. Even so, it is adequate for parametric studies concerning the influence of material properties and geometrical parameters. The geometrical parameters of the model are: the external size of the cubic cell (L_0), the radius of the particle (R_p) and

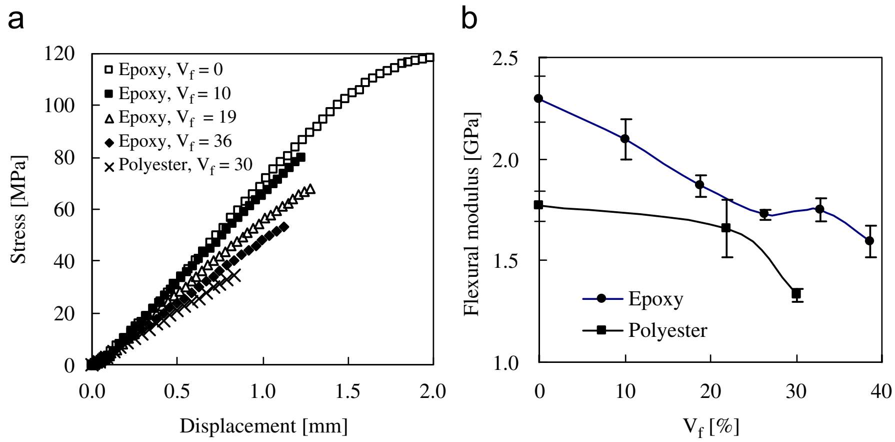

Fig. 1. (a) Typical stress–displacement curves in bending tests for different filler contents. (b) Influence of microsphere volume content on flexural modulus. (1 mm/min load rate.)

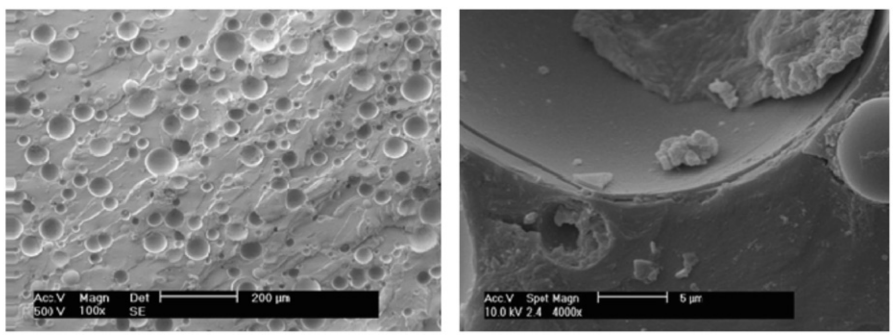

Fig. 2. (a) SEM photo of a fracture surface (V_f=26%) and (b) details of a broken particle.

the thickness of the wall (t_p). The particle's volume fraction (V_f) is the ratio between particle's volume ($4\pi R^3/3$) and the volume of the cubic cell (L_0^3). The hollow sphere and the matrix were assumed to be different homogeneous isotropic materials with linear elastic behaviour. The material properties considered for the epoxy matrix were E_m=2.3 GPa; υ_m=0.35, while for the glass particles, the properties assumed were E_g=85 GPa; υ_g=0.3. A model with two particles (Fig. 3b) was also considered to study the influence of the relative position of particles. The distance between the two particles is indicated by DP in Fig. 3b.

To determine the stiffness of the composite (E_c), a uniform displacement dx=0.1 mm was applied at one face of the cubic cell, while the opposite one was maintained fixed, as illustrated in Fig. 3. Young's modulus was calculated from

$$E_c = \frac{\sigma}{\varepsilon} = \frac{\sum R_x/A}{dx/L_0} \tag{2}$$

being σ the average stress, ε the strain, R_x the reaction force at the fixed face and A the corresponding area ($L_0 \times L_0$). The stiffness of the composite depends on several parameters, namely the rigidity of the matrix (E_m) and reinforcement (E_g), the radius (R_p) and the thickness (t_p) of hollow particles, and the volumetric fraction of particles (V_f)

$$E_c = \tilde{f}(E_g, E_m, R_p, t_p, V_f) \tag{3}$$

A non-dimensional version of this equation was developed, based on Buckingham's theorem of the non-dimensional analysis. Considering the stiffness of the matrix and particle's radius as the primary variables

$$\frac{E_c}{E_m} = \tilde{f}\left(\frac{E_g}{E_m}, \frac{t_p}{R_p}, V_p\right) \tag{4}$$

This physical model was implemented numerically using commercial finite element software. Fig. 4 shows the geometry of the unit cell, composed of a hollow particle and the matrix (only partially represented). The finite element mesh, also presented, is composed of 8-node isoparametric brick elements. The number of elements and nodes was 9408 and 10620, respectively. The model is quite flexible as it was developed parametrically in terms of particle size, wall's thickness, volumetric fraction and elastic properties of filler and matrix.

4. Numerical results

4.1. Validation of the numerical model

The numerical model was validated intrinsically considering a mesh refinement study and extrinsically compared with experimental results. The results obtained, presented in Fig. 5, show a convergence with mesh refinement and that stabilised values were obtained with 6912 elements. The model considered in subsequent studies has 9408 elements and is indicated in Fig. 5 by an arrow. Notice that the variation between maximum and stabilised stiffness is only 0.23% of the stabilised value, which indicates a low sensitivity to mesh size.

The minimum number of particles required to have a representative volume element was also studied. Models with one, 4 and 8 unit cells were studied, with a regular spatial distribution of particles, and minor variations were obtained of 0.15%. This is in accordance with findings of Drugan et al. [7], Drugan [8] and Kari et al. [9]. In order to minimise the numerical effort, only one particle was considered in subsequent studies.

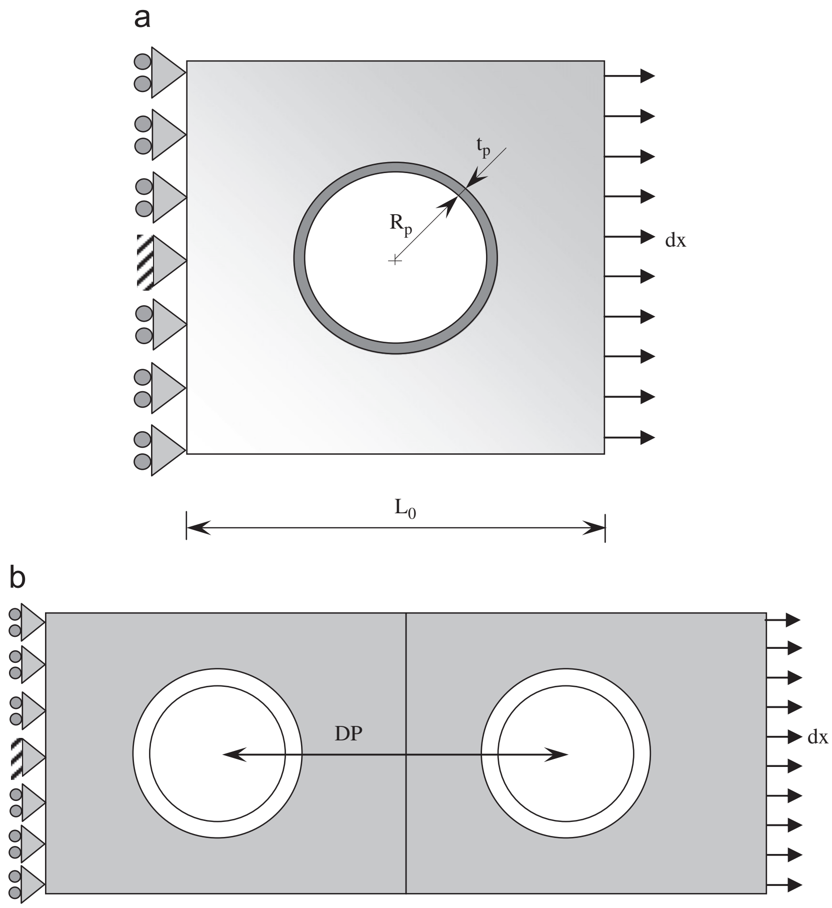

Fig. 3. Geometry and boundary conditions: (a) single particle model and (b) model with two particles.

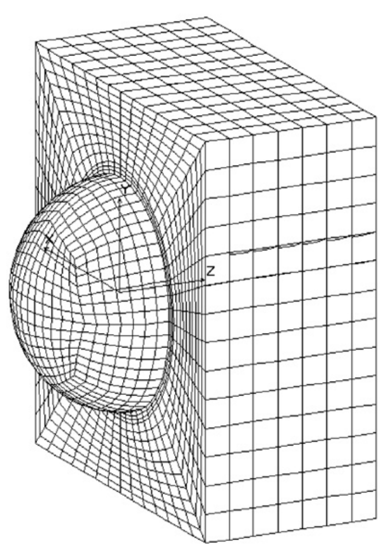

Fig. 4. Finite element model of a simple cubic cell.

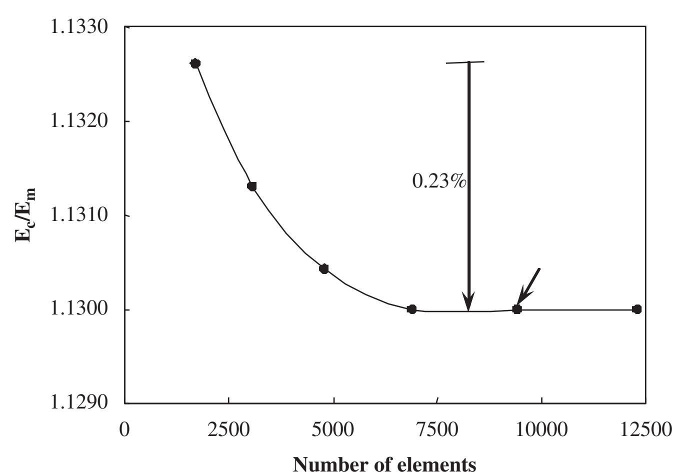

Fig. 5. Mesh refinement study (epoxy matrix, E_m=2.3 GPa, υ_m=0.35, E_g=85 GPa, υ_g=0.3; 1 unit cell, V_f=15%).

Fig. 6a compares experimental results obtained for an epoxy, with numerical predictions. Good agreement was obtained for R_p/t_p=120, which indicates that t_p=0.25 μm, assuming that R_p=30 μm, E_m=2300 MPa and E_g=85 GPa. The thickness measured in Fig. 2b was approximately 0.37 μm, which agrees well with the predicted value. Notice that real thickness is expected to have some scatter and that the elastic properties assumed may not be exact.

4.2. Parametric study

Fig. 6a presents the influence of particle volumetric fraction (V_f) on the stiffness for different thicknesses of hollow spheres. The non-dimensional stiffness, E_c/E_m being an E_m matrix's rigidity and an E_c composite's rigidity, approaches 1 for low values of V_f, as could be expected. Two trends are evident, depending of the thickness of hollow spheres (t_p). For relatively high values of t_p, the increase in V_f increases the stiffness of the composite, which indicates that the

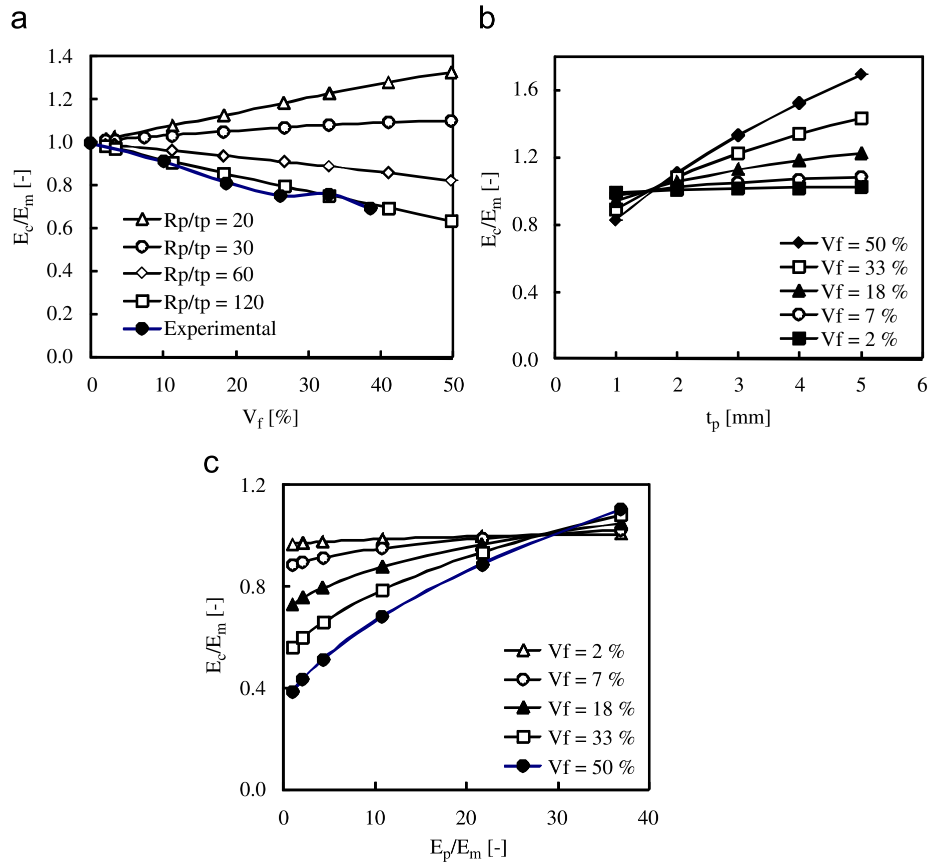

Fig. 6. Rigidity of the composite (E_c/E_m). (a) Effect of volume fraction of particles (V_f). (b) Effect of thickness of hollow spheres. (c) Effect of the particle's rigidity. (E_m=2.3 GPa, υ_m=0.35; υ_p=0.3, E_g=85 GPa, υ_g=0.3; 9408 el.s.)

particle is more rigid than the matrix. On the other hand, for relatively low values of t_p, the increase in V_f reduces the composite's stiffness, which indicates that the particle's stiffness is lower than the matrix. Notice that although the glass of hollow spheres is relatively stiff, a significant portion of each particle is air. Fig. 6b presents the influence of the particle's thickness (t_p) on an E_c/E_m. The increase in thickness increases the stiffness of the particle and therefore the stiffness of the composite. For small volume fractions of particles, the matrix controls the global stiffness; therefore, the variation of t_p has a small impact on an E_c/E_m. For relatively large volume fractions, the thickness has a major impact on an E_c/E_m. For a specific value of t_p, the rigidity of the particle equals the rigidity of the matrix; therefore, the volume fraction has no influence. Fig. 6c shows the influence of the rigidity of the material of the particle on the global rigidity. Once again, this parameter only has an influence for relatively large volume fractions.

4.3. Sensitivity analysis

A sensitivity analysis was developed to quantify the influence of the different parameters. A non-dimensional sensitivity can be defined as

$$\Delta f_{nd} = \frac{\partial E_c}{\partial x_i} \frac{x_i}{y} \tag{5}$$

with an E_c being the stiffness of the composite and x_i as one of the independent parameters, i.e., E_g, E_m, t_p, R_p or V_f. Notice that a sensitivity of 0.5 indicates that a variation of 1% in x_i produces a variation of 0.5% in an E_c. Fig. 7 presents the results obtained for the non-dimensional sensitivity (Δf_{nd}). The plot shows a large sensitivity to the matrix's stiffness (E_m). The sensitivities relatively to the stiffness of the particle (E_g), and to its thickness and radius (t_p, R_p) are similar. The lowest sensitivity was relatively to particle volume fraction. The increase in volume fraction increases the importance of the particle's parameters (E_g, t_p, R_p, V_f), and decreases the sensitivity to the matrix, as could be expected. Finally, the sensitivities vary linearly with the particle's volume fraction.

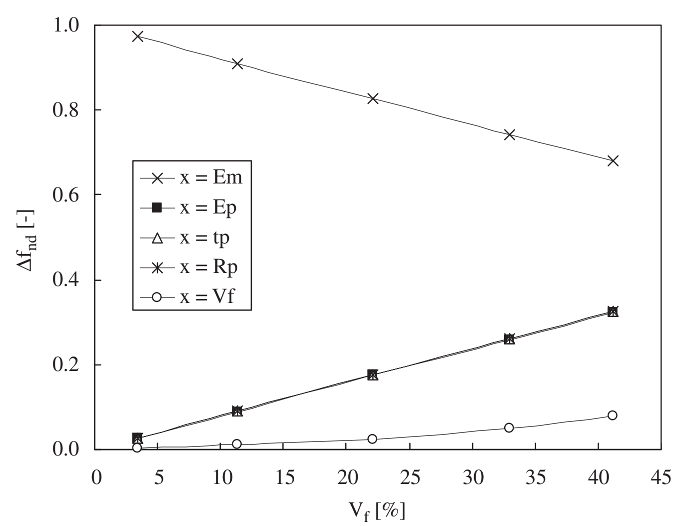

Fig. 7. Non-dimensional sensitivity relatively to E_m, E_p, t_p, R_p and V_f. (Epoxy matrix, E_m=2.3 GPa, υ_m=0.35; υ_p=0.3, E_g=85 GPa, υ_g=0.3; t_p=0.37 μm; R_p=30 μm;1 unit cell, 9408 el.s.)

4.4. Interpolation

A numerical procedure based on FEM shape functions was used to predict the stiffness for an arbitrary combination of material and geometrical parameters. The parametric space ($1<E_g/E_m<37$; $0.02<V_f<0.50$; $12<R_p/t_p<60$) was divided into 160 linear finite elements and 270 nodes. The finite elements had a parallelepiped shape, as illustrated in Fig. 8a. Fig. 8b shows the division of the E_g/E_m-V_f space. The nodal values of E_c/E_m were obtained with the finite element method described in Section 3. Finally, for intermediate parameters, the stiffness was predicted by linear interpolation, using the shape functions

$$E_c/E_m=\sum_{i=1}^{8} N_i(E_c/E_m)_i \tag{6}$$

where N_i is the shape function of node i in local coordinates written as

$$N_i(\xi,\eta,\zeta)=\frac{1}{8}(1+\xi\xi_i)(1+\eta\eta_i)(1+\zeta\zeta_i)\quad(\xi_i,\eta_i,\zeta_i=-1,+1) \tag{7}$$

This interpolation procedure has several advantages, namely, an easier implementation and extension of parametric region as well as an automatic definition of interpolation limits. The elements may have distinct sizes with refinements in regions of important gradients. On the other hand, this method cannot be used for extrapolation and a small error is introduced as a result of assuming linear variations within the elements. The model developed in this work may be used in designs by selecting the volume fraction and particle size, which gives a specific stiffness.

This numerical model was used to predict the critical values of glass stiffness (E_g), the hollow particles radius (R_p) and the thickness (t_p), such that the particle's rigidity equaled the matrix's rigidity. Fig. 9 shows that the increase in the particle's rigidity must be compensated by the increase in R_p/t_p, i.e., by the increase in R_p or by the decrease in t_p. Notice that the volume fraction has no influence on this "magic" value. The following equation was obtained by the numerical regression:

$$\frac{R_p}{t_p}=0.0141\left(\frac{E_g}{E_m}\right)^2+0.4578\frac{E_g}{E_m}+7.0838 \tag{8}$$

and is valid for $16<R_p/t_p<43$. Filling particles are usually stiffer and more resistant than the matrix; however, the region below curve does not follow this trend. The dashed line in Fig. 9 was obtained with Voigt model, $E_p=E_g\times V_g$, where E_p is the particle's stiffness, E_g is the glass's stiffness and V_g is the volume fraction of glass in the particle. The model that was developed calculates the stiffness of the particle considering only the volume of the material with no influence of shape. The difference between the two curves in Fig. 9 indicates that the hollow spheres are an efficient geometry in terms of stiffness. Finally, Fig. 9 shows the particles K15, S22 and K37 described in Bardella and Genna [2], as having the average dimensions indicated in Table 1. Particles K15 and S22 are more flexible than the matrix, particularly K15. On the other hand, K37 particles are stiffer than the epoxy matrix.

The interpolation model was also applied to predict the stiffness of composites with particles K15, S22 and K37, described in Bardella and Genna [2]. The properties considered for the epoxy matrix were $E=2.8$ GPa, $\nu=0.41$, and for the glass of hollow spheres were $E=70.11$ GPa, $\nu=0.23$. Fig. 10 compares the results of the interpolation model developed here with the numerical results of Bardella and Genna [2]. An excellent agreement is obvious, reinforcing the strength of the interpolation model. Additionally, this agreement validates the use of axisymmetric models in the single-particle analysis. Notice that for particles K15 and S22, the increase in volume fraction decreases the stiffness of the

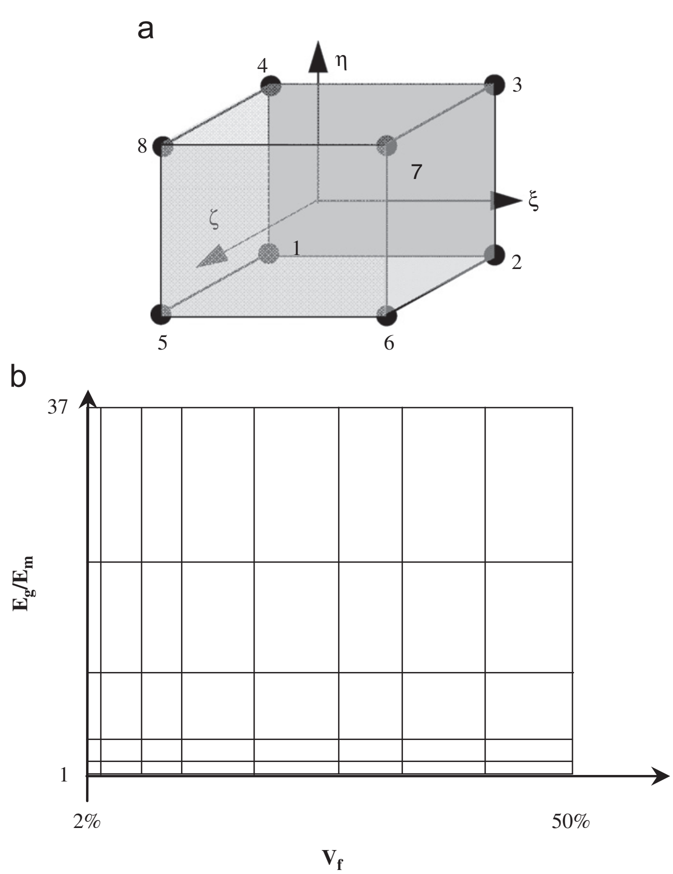

Fig. 8. (a) Linear finite element and (b) division of E_p/E_m-V_f space.

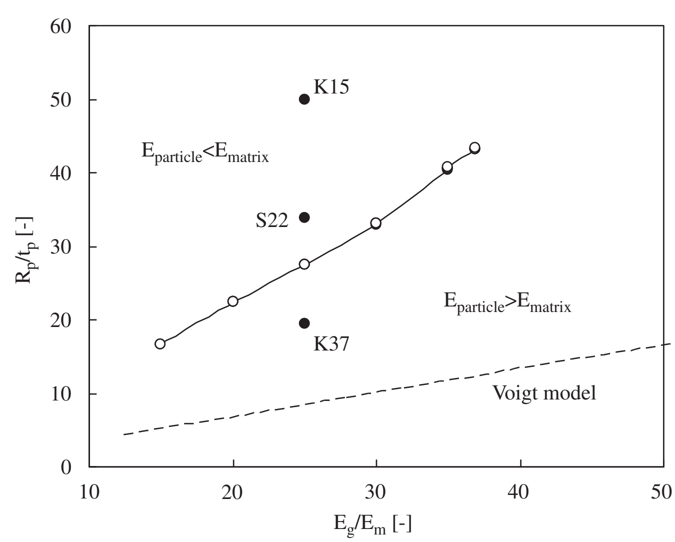

Fig. 9. Values of E_c/E_m and R_p/t_p, such that the global rigidity of the particle equals the rigidity of matrix.

Table 1
Properties of hollow spheres, according to Bardella et al. (2001).

	R_p [μm]	t_p [μm]	R_p/t_p
K15	35	0.7	1.8
S22	20	0.59	1.2
K37	25	1.28	0.7

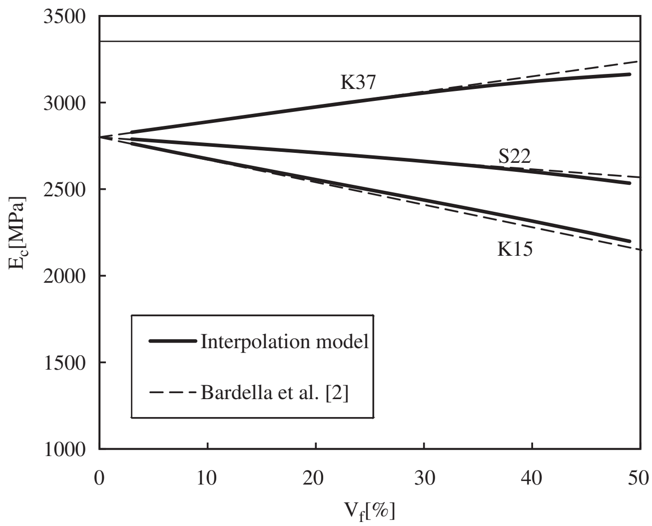

Fig. 10. Validation of interpolation model with the literature results.

composite, which indicates that the particles are less rigid than the matrix. The opposite trend is observed for the K37 particles. Notice also that $E_p/E_m=25$; therefore, the critical value of R_p/t_p is 27.4 according to Eq. (8). The composite with K37 particles has a value of R_p/t_p lower than the critical value; therefore, the composite is less stiff than the matrix. The opposite behaviour is observed for K15 and S22 particles.

5. Conclusions

The flexural properties of syntactic foams with epoxy and polyester resins were determined. The flexural stiffness decreases with filler volume fraction, but the specific value is only marginally affected. Specific properties of filled polyester foams are lower than for epoxy based foams. A numerical model with a single-particle was developed to study the influence of the matrix (E_m) and reinforcement (E_g), the radius (R_p) and thickness (t_p) of hollow particles and the volumetric fraction of particles (V_f). The global rigidity of the particle equals the rigidity of the matrix for specific values of particle size, thickness and rigidity. In this case, the composite's rigidity is independent of the volume fraction. A sensitivity analysis was developed to understand the influence of different parameters. The matrix's stiffness must be accurately determined, because it has the most influence in the model.

A numerical procedure based on FEM shape functions was used to interpolate the rigidity values. This model was used to identify the values of E_c/E_m and R_p/t_p such that global rigidity of the particle equals the rigidity of the composite's matrix. The model developed can be used in a design, by selecting the volume fraction and particle size to give a specific rigidity. The model used in this study to predict the rigidity of syntactic foams was verified through comparison with results found in the literature.

References

[1] E. Rizzi, E. Papa, A. Corigliano, Mechanical behaviour of a syntactic foam: experiments and modelling, International Journal of Solids and Structures 37 (2000) 5773–5794.
[2] L. Bardella, F. Genna, On the elastic behaviour of syntactic foams, International Journal of Solids and Structures 38 (2001) 7235–7260.
[3] H.S. Kim, M.A. Khamis, Fracture and impact behaviours of hollow micro-spheres/epoxy resin composites, Compos. Part A: Appl. Sci. Manuf. 32 (2001) 1311–1317.
[4] S. Li, A. Wongsto, Unit cells for micromechanical analyses of particle-reinforced composites, Mech. Mater. 36 (2004) 543–572.
[5] C.P. Tsui, C.Y. Tang, T.C. Lee, Finite element analysis of polymer composites filled by interphase coated particles, Journal of Materials Processing Technology 117 (2001) 105–110.
[6] I. Balac, M. Milovancevic, C-y Tang, P.S. Uskokovic, D.P. Uskokovic, Estimation of elastic properties of a particulate polymer composite using a face-centered cubic FE model, Mater. Lett. 58 (2004) 2437–2441.
[7] W.J. Drugan, J.R. Willis, A micromechanics-based nonlocal constitutive equation and estimates of the representative volume element size for elastic composites, J. Mech. Phys. Solids 44 (1996) 497–524.
[8] W.J. Drugan, Micromechanics-based variational estimates for a higher-order nonlocal constitutive equation and optimal choice of effective moduli of elastic composites, J. Mech. Phys. Solids 48 (2000) 1359–1387.
[9] S. Kari, H. Berger, R. Rodriguez-Ramos, U. Gabbert, Computational evaluation of effective material properties of composites reinforced by randomly distributed spherical particles, Compos. Struct. 77 (2007) 223–231.
[10] J. Segurado, J. Llorca, A numerical approximation to the elastic properties of sphere-reinforced composites, J. Mech. Phys. Solids 50 (2002) 2107–2121.
[11] J. Segurado, C. González, J. Llorca, A numerical investigation of the effect of particle clustering on the mechanical properties of composites, Acta Materialia 51 (2003) 2355–2369.
[12] J. Segurado, J. LLorca, Computational micromechanics of composites: the effect of particle spatial distribution, Mech. Mater. 38 (2006) 873–883.
[13] L.L. Mishnaevsky Jr., Three-dimensional numerical testing of microstructures of particle reinforced composites, Acta Materialia 52 (2004) 4177–4188.
[14] J. Segurado, J. Llorca, A computational micromechanics study of the effect of interface decohesion on the mechanical behavior of composites, Acta Materialia 53 (2005) 4931–4942.
[15] A. Eckschlager, W. Han, H.J. Bohm, A unit cell model for brittle fracture of particles embedded in a ductile matrix, Comput. Mater. Sci. 25 (2002) 85–91.
[16] C.P. Tsui, D.Z. Chen, C.Y. Tang, P.S. Uskokovic, J.P. Fan, X.L. Xie, Prediction for debonding damage process and effective elastic properties of glass-bead-filled modified polyphenylene oxide, Compos. Sci. Technol. 66 (2006) 1521–1531.
[17] O. Pierard, C. González, J. Segurado, J. LLorca, I. Doghri, Micromechanics of elasto–plastic materials reinforced with ellipsoidal inclusions, Int. J. Solids Struct. 44 (2007) 6945–6962.
[18] O. Pierard, J. LLorca, J. Segurado, I. Doghri, Micromechanics of particle-reinforced elasto-viscoplastic composites: finite element simulations versus affine homogenization, Int. J. Plasticity 23 (2007) 1041–1060.
[19] L. Mishnaevsky Jr., M. Dong, S. Honle, S. Schmauder, Computational mesomechanics of particle-reinforced composites, Comput. Mater. Sci. 16 (1999) 133–143.
[20] N. Chawla, R.S. Sidhu, V.V. Ganesh, Three-dimensional visualization and microstructure-based modelling of deformation in particle-reinforced composites, Acta Materialia 54 (2006) 1541–1548.
[21] P.R. Marur, Effective elastic moduli of syntactic foams, Mater. Lett. 59 (2005) 1954–1957.